CH Stretching Overtone Spectra of Fluorine Substituted Toluenes†

Zimei Rong, Chenxi Zhu, and Bryan R. Henry*

Department of Chemistry and Biochemistry, University of Guelph, Guelph, Ontario N1G 2W1, Canada

Received: May 8, 2003; In Final Form: September 23, 2003

We have measured and analyzed the vapor phase CH stretching overtone spectra of 3,5-difluorotoluene, 2,3,5,6-tetrafluorotoluene, and 2,3,4,5,6-pentafluorotoluene. The aryl bands are complex due to Fermi resonance. We have used a two-level system model to analyze the Fermi resonance within the aryl bands. The aryl regions of the overtone spectra are "corrected" for Fermi resonance and interpreted as uncoupled stretching oscillators. The methyl band profiles are complex due to the coupling between CH stretching and methyl torsion. The methyl band profiles are simulated with a CH stretching methyl torsion model. The CH stretching modes are described by a harmonically coupled anharmonic oscillator local mode model, and the methyl torsion is described by a rigid rotor model. Simulation parameters are obtained from ab initio calculations with the HF/6-31G(d) method. Relative intensities of aryl and methyl contributions in the CH stretching overtone spectra in the region $\Delta\nu_{CH} = 2-5$ are measured and calculated for these molecules. We have found that the methyl bands of 3,5-difluorotoluene are very similar to corresponding bands in toluene, 4-methylpyridine, *p*-xylene, and *m*-xylene. The methyl bands of 2,3,5,6-tetrafluorotoluene and 2,3,4,5,6-pentafluorotoluene are virtually identical to those of 2,6-difluorotoluene. Thus, the main factor that determines the structure in methyl CH stretching overtone spectra of these molecules is the nature of the groups adjacent to the methyl group. The aryl bands of these molecules are primarily affected by the nearest substituents.

Introduction

The local mode model, as its name implies, concentrates on a pair of adjacent atoms, which is treated as an isolated oscillator.[1,2] A pure stretching local mode model describes the stretching of a pair of XH atoms in a molecule. However, a pure stretching local mode model cannot always explain even the stretching overtone spectra due to the interaction between stretching modes and other vibrational modes. Interoscillator coupling between stretches was included in the harmonically coupled anharmonic oscillator (HCAO) local mode model.[3−7] This coupling is significant at lower overtones and becomes weaker as the stretching vibrational quantum number increases. This model was successful for explaining XH stretch−stretch coupling in overtone spectra such as the CH_2 stretching overtones of dihalomethanes.[4−7]

Coupling between CH stretching and methyl internal rotation was introduced to interpret methyl stretching overtone spectra.[8−10] We have formulated a CH stretching methyl torsion model and used it to explain successfully methyl overtone spectra for a series of molecules.[11−15] In this model, CH stretching modes are described by the HCAO local mode model, and methyl torsion is described by a rigid rotor model. The stretching torsion coupling affects all overtones if the torsional potential is sufficiently low. In our previous studies, we found the methyl overtone spectra of toluene, 4-methylpyridine, *p*-xylene, and *m*-xylene with quasi free rotors are very similar.[12−14,16] The methyl overtone spectrum of 2,6-difluorotoluene is different from the spectra of the above molecules although the torsional potential of 2,6-difluorotoluene is still relatively low.[11]

Fermi resonance extensively exists in stretching overtone spectra and has been quantitatively analyzed in different approaches.[10,17−23] Unperturbed stretching energies with Fermi resonance were obtained from interpolation and extrapolation of the Birge−Sponer plot where the stretching mode parameters are obtained from the Birge−Sponer fit of the transitions without obvious Fermi resonance.[19,20] Winther et al. suggested three methods to obtain the unperturbed frequencies from the perturbed frequencies at the fundamental transition for dicyanoaccetylene.[23] One of their methods obtains unperturbed frequencies from the intensity ratio and the corresponding perturbed frequencies.[22,23] Our approach is similar in that we obtain the unperturbed frequencies from the perturbed frequencies and relative intensities for overtones in a two-level system model. Then, we will interpret the aryl CH stretching overtone spectra with an uncoupled stretching oscillator model.

In this paper we will study the effect of chemical environment on CH stretching overtone spectra. We will attempt to understand the range over which the environment can affect the overtone spectra of a given group. Is the environment effect "local", and how "local" is it? Methyl band profiles of 2,3,5,6-tetrafluorotoluene and 2,3,4,5,6-pentafluorotoluene are suitable for such comparisons.[24] We will analyze the methyl and aryl CH stretching overtone spectra of toluene, 3,5-difluorotoluene, 2,6-difluorotoluene, 2,3,5,6-tetrafluorotoluene, and 2,3,4,5,6-pentafluorotoluene. We will observe how the substituents affect both the methyl and aryl bands in the CH stretching overtone spectra of these molecules.

Experimental Section

2,3,5,6-Tetrafluorotoluene and 2,3,4,5,6-pentafluorotoluene with purities of 99% were obtained from Aldrich Inc. The samples were used without further purification except for a freeze−pump−thaw procedure with liquid nitrogen. 3,5-Difluorotoluene was synthesized from α-bromo-3,5-difluorotoluene with a lithium hydride reaction in our laboratory by David M. Turnbull. The ether impurity was eliminated by several distil-

† Part of the special issue "Charles S. Parmenter Festschrift".

10.1021/jp0305887 CCC: $25.00
Published on Web 10/29/2003

lations, and the remaining impurities were negligible. The absence of detectable impurity was verified with NMR spectra.

The room-temperature vapor phase overtone spectra of these substituted toluenes were recorded in the $\Delta v_{CH} = 2$ and 3 regions with a Cary-5e conventional absorption spectrometer. A Wilks variable path length (maximum 20.25 m) cell was used to record the overtone spectra. The sample flask was opened long enough for the vapor to reach equilibrium in the Wilks cell. The cell was pumped down and rinsed several times with nitrogen after a sample spectrum was recorded. Then, a background spectrum was taken after a good vacuum (below 100 mTorr) was achieved in the cell. The absorption spectrum was obtained by subtracting the background from the sample spectrum.

The room-temperature vapor phase overtone spectra of these substituted toluenes were recorded in the $\Delta v_{CH} = 4-6$ region by intracavity laser photoacoustic spectroscopy (ICL-PAS) with an accuracy of 1 cm^{-1}. Our version of ICL-PAS has been described elsewhere.[25,26] An argon ion laser (Coherent Innova 200) pumped titanium/sapphire solid-state broad band tunable laser (Coherent 890) was used to record the $\Delta v_{CH} = 4$ region (with midwave optics) and the $\Delta v_{CH} = 5$ region (with short-wave optics), respectively. In these two regions, we recorded the overtone spectra of 2,3,5,6-tetrafluorotoluene and 2,3,4,5,6-pentafluorotoluene without a buffer gas. We used an argon buffer gas to record the overtone spectrum of 3,5-difluorotoluene. Typically the cell was pumped overnight to reach a background pressure of 10^{-5} Torr. The sample was passed through a column filled with dry molecular sieves to eliminate trace water. However, we still observe weak water lines which were used to calibrate the overtone spectra. In the $\Delta v_{CH} = 6$ region, a tunable dye laser (Coherent 599) was used. A dye, which covers both the methyl and aryl regions, was not available. The DCM and R6G laser dyes were used to record the overtone spectra in the methyl and aryl regions, respectively. Due to the weak photoacoustic signal in the $\Delta v_{CH} = 6$ region, an argon buffer gas was used to improve the signal. Direct addition of the buffer gas was unsuccessful. Both the sample gas and buffer gas (100 Torr) were passed through columns of molecular sieves into a mixing bowl, where they were stirred for 1−2 h before filling the cell.

The overtone spectra were decomposed into component peaks with a deconvolution program within GRAMS AI.[27] The spectra were deconvoluted into a number of Lorentzian profiles and a linear baseline.

Theory and Calculations

The oscillator strength of a vibrational transition from the ground state to a vibrationally excited state within the same electronic state is given by[28]

$$f = \frac{4\pi m_e}{3e^2\hbar}\tilde{\nu}_{eg}|\langle v|\vec{\mu}|0\rangle|^2 \tag{1}$$

where $\tilde{\nu}_{eg}$ is the transition frequency, $|0\rangle$ and $|v\rangle$ are the ground- and excited-state wave functions, $\vec{\mu}$ is the dipole moment function, $\hbar$ is the Planck constant, and m_e and e are the mass and the charge of an electron, respectively. Wave functions are obtained from the Hamiltonian, and dipole moment functions are calculated ab initio (vide infra).

CH Stretching Local Mode Model. The Hamiltonian of an aryl CH stretching oscillator can be expressed in a Morse wave function $|v\rangle$ basis set as

$$H/hc = \tilde{\omega}\left(v + \frac{1}{2}\right) - \tilde{\omega}x\left(v + \frac{1}{2}\right)^2 \tag{2}$$

where $\tilde{\omega}$ is the frequency in inverse centimeters, $\tilde{\omega}x$ is the anharmonicity in inverse centimeters, and v is the vibrational quantum number of the oscillator. The frequency and anharmonicity of the oscillator can be obtained by a Birge−Sponer fitting of overtone peak positions $\tilde{\nu}$ as[7,29]

$$\tilde{\nu}/v = \tilde{\omega} - (v+1)\tilde{\omega}x \tag{3}$$

A pure CH stretching band cannot always be resolved because of spectral band overlap or coupling to other modes. The CH oscillator frequency and anharmonicity can be obtained from the ab initio calculations. The ab initio frequency and anharmonicity also provide a helpful guide in the analysis of overtone spectra. The frequency and anharmonicity in inverse centimeters as functions of the second-order potential energy coefficient V_2 in hartree per square angstrom and the third-order potential energy coefficient V_3 in hartree per cubic angstrom for a CH stretching oscillator are expressed as[30,31]

$$\tilde{\omega} = 3990\ [\mathrm{cm^{-1}\cdot \AA \cdot hartree^{-1/2}}] \times \sqrt{V_2} \tag{4}$$

$$\tilde{\omega}x = 18.13\ [\mathrm{cm^{-1}\cdot \AA^2}] \times \left(\frac{V_3}{V_2}\right)^2 \tag{5}$$

The x component of the dipole moment function can be written as

$$\mu_x(q) = \sum_{i=0}^{6} a_i q^i \tag{6}$$

where the a_i are Taylor series expansion coefficients. The y and z components are written in a similar fashion. We have shown that the dipole moment function limited to sixth order is sufficient for calculation of overtone intensity up to $\Delta v_{CH} = 6$.[32] A 15 point grid from −0.3 to 0.4 Å with 0.05 Å steps is used to calculate the dipole moment function for an aryl CH stretching oscillator. A 9 point grid from −0.2 to 0.2 Å is used to calculate the frequency and anharmonicity. The ab initio calculations are carried out at the geometry optimized structure with Gaussian 98.[33]

Fermi Resonance. Fermi resonance between stretching and bending was found in the aryl bands of these fluorine substituted toluenes. We use a two-level system model to obtain uncoupled stretching frequencies from these aryl bands.

We assume an unperturbed two-level system, a pure CH stretching state s_1 with an energy $\tilde{\nu}_1$ (cm^{-1}), and a combination state c_2 with an energy $\tilde{\nu}_2$ (cm^{-1}). The zero point energies have been subtracted from the energies $\tilde{\nu}_1$ and $\tilde{\nu}_2$. The state s_1 and state c_2 are coupled with the coupling energy γ (cm^{-1}). The perturbed energies $\tilde{\nu}_+$ and $\tilde{\nu}_-$ and wave functions $|+\rangle$ and $|-\rangle$ can be obtained from the unperturbed energies $\tilde{\nu}_1$ and $\tilde{\nu}_2$, and the coupling energy γ as[34]

$$\tilde{\nu}_\pm = \frac{\tilde{\nu}_1 + \tilde{\nu}_2}{2} \pm \sqrt{\gamma^2 + \left(\frac{\tilde{\nu}_1 - \tilde{\nu}_2}{2}\right)^2} \tag{7}$$

The perturbed wave functions are[34]

$$|+\rangle = a|s_1\rangle + b|c_2\rangle \tag{8}$$

$$|-\rangle = -b|s_1\rangle + a|c_2\rangle \tag{9}$$

where the normalized coefficients a and b are obtained from the parameters $\tilde{\nu}_1$, $\tilde{\nu}_2$, and γ. The unperturbed energies are expressed as

$$\tilde{\nu}_1 = a^2\tilde{\nu}_+ + b^2\tilde{\nu}_- \tag{10}$$

$$\tilde{\nu}_2 = b^2\tilde{\nu}_+ + a^2\tilde{\nu}_- \tag{11}$$

The transition intensity from the ground state to the unperturbed combination state is assumed to be zero. Then, the relationship between the oscillator strengths of the transitions $|0\rangle \rightarrow |+\rangle$, f_+, and $|0\rangle \rightarrow |-\rangle$, f_-, and the wave function coefficients is given by

$$\frac{f_+}{f_-} = \frac{\tilde{\nu}_+ a^2}{\tilde{\nu}_- b^2} \tag{12}$$

Finally, the unperturbed energies are obtained from spectral parameters, peak positions, and oscillator strengths, as

$$\tilde{\nu}_1 = \frac{(f_+ + f_-)\tilde{\nu}_+\tilde{\nu}_-}{f_+\tilde{\nu}_- + f_-\tilde{\nu}_+} \tag{13}$$

$$\tilde{\nu}_2 = \frac{f_+\tilde{\nu}_-\tilde{\nu}_- + f_-\tilde{\nu}_+\tilde{\nu}_+}{f_+\tilde{\nu}_- + f_-\tilde{\nu}_+} \tag{14}$$

Relative oscillator strengths, which are required in the calculation, can be measured more accurately than absolute oscillator strengths. The following approximation may be used,[19]

$$\frac{f_+}{f_-} = \frac{a^2}{b^2} \tag{15}$$

Then, we have the simpler formulas

$$\tilde{\nu}_1 = \frac{f_+\tilde{\nu}_+ + f_-\tilde{\nu}_-}{f_+ + f_-} \tag{16}$$

$$\tilde{\nu}_2 = \frac{f_+\tilde{\nu}_- + f_-\tilde{\nu}_+}{f_+ + f_-} \tag{17}$$

The differences between the unperturbed frequencies from eqs 13 and 14 and from eqs 16 and 17 are very small (vide infra). However, the physical meaning of eqs 16 and 17 is more straightforward. For example, eq 16 indicates that, in a two-level system model, the unperturbed frequency is the average of the perturbed frequencies weighted with the corresponding relative oscillator strengths. From this analysis the uncoupled stretching transition frequencies can be found, which leads to the local mode frequency and anharmonicity from the Birge−Sponer fit.[29] From eq 16 we have an interesting deduction

$$\tilde{\nu}_+ - \tilde{\nu}_1 = \frac{f_-}{f_+ + f_-}(\tilde{\nu}_+ - \tilde{\nu}_-) \tag{18}$$

The difference between the perturbed and unperturbed stretching frequencies is the difference of perturbed frequencies multiplied by the relative perturbed combination band intensity.

CH Stretching Methyl Torsion Model. For completeness we summarize the previously published model here.[13,14] The CH stretching methyl torsion model describes CH stretching modes within the HCAO local mode model and methyl torsion modes in a rigid rotor model. The Hamiltonian and the dipole moment function of the methyl group, including both CH stretching and methyl torsion, are described within a methyl coordinate system.[13,14] The coordinate system is fixed to the ring frame with the z axis defined along the C−C bond, around which the methyl group rotates, from the carbon atom on the ring toward the methyl carbon atom. The x-axis is in the ring plane (xz plane) with the positive x-axis direction toward the methyl hydrogen atom (H_1). The hydrogen atom at positive y is numbered as the second hydrogen atom (H_2). The torsional angles of CH bonds are defined as the corresponding dihedral angle with respect to the ring plane. In a rigid rotor assumption, the relationships between the three torsional angles are $\theta_2 = \theta_1 + 2\pi/3$ and $\theta_3 = \theta_1 - 2\pi/3$.

The Hamiltonian for a rotating methyl group is described in a stretching torsion basis set as products of Morse wave functions and rigid rotor wave functions. Thus, the Hamiltonian is given by[13,14]

$$H_{v_1v_2v_3}/hc = \sum_{i=1}^{3}\left[\Omega F_i\left(v_i + \frac{1}{2}\right) - XF_i\left(v_i + \frac{1}{2}\right)^2\right] + VF_1 + Bm^2 - \gamma'(a_1a_2^+ + a_1^+a_2 + a_2a_3^+ + a_2^+a_3 + a_3a_1^+ + a_3^+a_1) \tag{19}$$

where $F_i = [1, \cos(\theta_i), ..., \cos(6\theta_i), \sin(\theta_i), ..., \sin(6\theta_i)]^T$ are Fourier series components in a column with a dimension of 13, and $\mathbf{V}$, $\mathbf{\Omega}$, and $\mathbf{X}$ are vectors consisting of the Fourier series expansion coefficients for the potential, frequency, and anharmonicity. γ' is the effective CH stretch−stretch coupling constant. a and a^+ are the ladder operators of harmonic oscillators. B is the rotational constant of the methyl group. This Hamiltonian will be diagonalized to obtain the wave functions and energy levels; in other words, we will not invoke an adiabatic approximation in obtaining a solution.

The methyl dipole moment function is approximated by a series expansion in the CH stretching coordinates and the torsional angle.[13,14] The permanent dipole moment is not included, since it does not contribute to the vibrational transition intensities. Thus, the x component of the dipole moment vector becomes[13,14]

$$\mu_x = \sum_{i=1}^{3} Q_i C_x F_i \tag{20}$$

where $Q_1 = [q_1, q_1^2, q_1^3, q_1^4, q_1^5, q_1^6, q_2q_3, q_2^2q_3, q_2q_3^2]$. The Q_2 and Q_3 vectors are obtained from Q_1 by permutation of the appropriate indices. The Fourier series column vectors F_i are defined in expressing the Hamiltonian. The dipole moment function expansion coefficients are tabulated in the 9×13 matrix $\mathbf{C}_x$. The y and z components of the dipole moment vector are obtained in a similar fashion with the expansion coefficient matrixes, $\mathbf{C}_y$ and $\mathbf{C}_z$, respectively.

The coefficient matrixes $\mathbf{V}$, $\mathbf{\Omega}$, $\mathbf{X}$, $\mathbf{C}_x$, $\mathbf{C}_y$, and $\mathbf{C}_z$ are obtained from 340 ab initio calculations. Initially, at each torsional angle, the molecular geometry is optimized at a fixed torsional angle. Then, we calculate the energy and dipole moment with a 15 point grid of the CH_1 bond from −0.3 to 0.4 Å in 0.05 Å steps. The Taylor series expansion coefficients of the dipole moment function are obtained from the 15 grid points with a sixth-order least-squares fit. We use 9 points from −0.2 to 0.2 Å with a sixth-order least-squares fit to calculate the second- and third-order energy derivative coefficients, from which we calculate the frequency and anharmonicity. We repeat these calculations for each 10°, rotating from 0° to 180°. The angular dependences

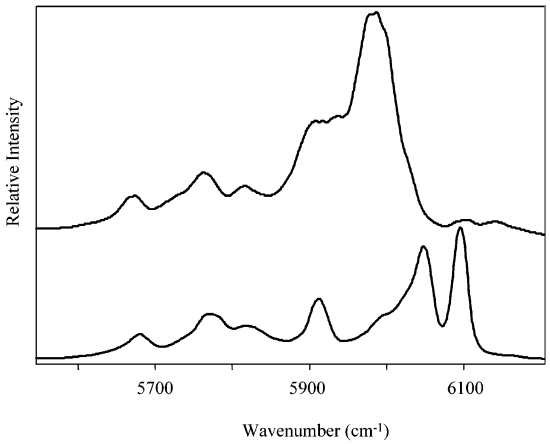

Figure 1. Room-temperature vapor phase overtone spectra of 3,5-difluorotoluene (bottom) and toluene (top) in the $\Delta v_{CH} = 2$ region. The spectra are rescaled to have similar magnitudes of methyl bands and are offset for clarity. The 3,5-difluorotoluene spectrum was measured with a path length of 20.25 m and a pressure of 13 Torr. The toluene spectrum is taken from ref 35.

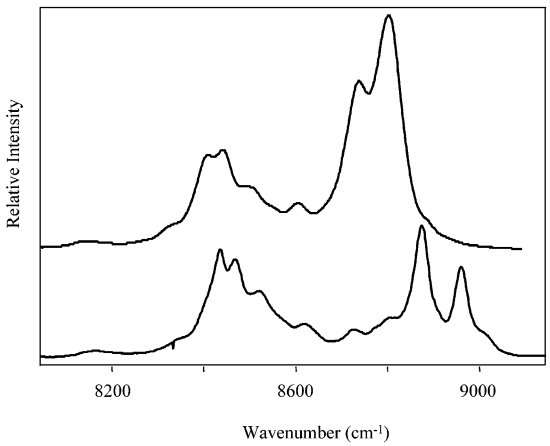

Figure 2. Room-temperature vapor phase overtone spectra of 3,5-difluorotoluene (bottom) and toluene (top) in the $\Delta v_{CH} = 3$ region. The spectra are rescaled to have similar magnitudes of methyl bands and are offset for clarity. The 3,5-difluorotoluene spectrum was measured with a path length of 20.25 m and a pressure of 13 Torr. The toluene spectrum is taken from ref 35.

of the dipole moment function, frequency, and anharmonicity Taylor expansion coefficients are calculated by fitting each in turn to a sixth-order Fourier series. The *B* values are calculated when the torsional angle is 0°.

For the torsional angles 0°, 90°, and 180°, a two-dimensional 5×5 grid with a 0.05 Å step size is calculated. The dipole moment Taylor expansion coefficients for the q_1q_2, $q_1q_2^2$, and $q_1^2q_2$ terms are determined from these two-dimensional grids with a third-order least-squares fit. The γ' value is calculated with the two-dimensional grid at 0°. The Fourier series coefficients for the Taylor series coefficients are obtained by solving a system of linear equations. The Hartree−Fock (HF) level of theory and the 6-31G(d) basis set are used in all ab initio calculations with Gaussian 98.[33]

When we simulated the methyl band profiles, each transition was approximated by a Lorentzian profile with a fwhm (full width at half maximum) of 20, 20, 20, and 30 cm^{-1} for $\Delta v_{CH} = 3-6$, respectively. In the vibrational ground state, the population of torsional states follows a Boltzmann distribution;[11] therefore, an *m* value up to 12 is adopted in eq 19.

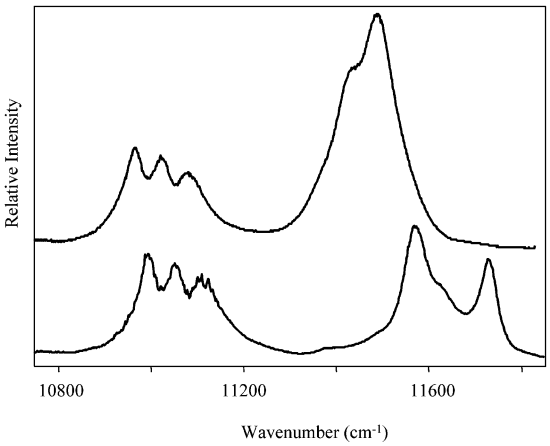

Figure 3. Room-temperature vapor phase overtone spectra of 3,5-difluorotoluene (bottom) and toluene (top) in the $\Delta v_{CH} = 4$ region. The spectra are rescaled to have similar magnitudes of methyl bands and are offset for clarity. The 3,5-difluorotoluene spectrum was measured by ICL-PAS with a pressure of 15 and 100 Torr of argon buffer gas. The toluene spectrum is taken from ref 35.

Results and Discussion

The room-temperature vapor phase overtone spectra of 3,5-difluorotoluene and toluene in the CH stretching regions corresponding to $\Delta v_{CH} = 2-6$ are shown in Figures 1−5. The overtone spectrum of toluene from the previous work is shown for comparison.[35] The overtone spectra in the regions $\Delta v_{CH} = 2$ and 3 were recorded with a conventional absorption spectrometer, and intensity is expressed as absorbance. However, here we are interested in relative intensity for visual comparison. These spectra have been offset for clarity and rescaled to have similar magnitudes of methyl bands. The methyl regions of the overtone spectra are very similar for 3,5-difluorotoluene and toluene, except at $\Delta v_{CH} = 3$. In the region of $\Delta v_{CH} = 3$, the lowest energy side peak is the strongest one for 3,5-difluorotoluene, whereas the strongest peak is the second lowest energy side peak for toluene (Figure 2). The methyl region and aryl region are overlapped at $\Delta v_{CH} = 2$ for the overtone spectra of toluene. Compared to the overtone spectrum of toluene, the overtone spectrum of 3,5-difluorotoluene is blue shifted with the aryl bands shifting more significantly.

The room-temperature vapor phase overtone spectra of 2,3,4,5,6-pentafluorotoluene, 2,3,5,6-tetrafluorotoluene, and 2,6-difluorotoluene in the CH stretching regions corresponding to $\Delta v_{CH} = 2-6$ are shown in Figures 6−10. The overtone spectrum of 2,6-difluorotoluene from the previous work is shown for comparison.[11] These spectra have been offset for clarity and rescaled to have similar magnitudes of methyl bands and the $\Delta v_{CH} = 6$ aryl band. The methyl regions of the overtone spectra of 2,3,4,5,6-pentafluorotoluene, 2,3,5,6-tetrafluorotoluene, and 2,6-difluorotoluene are very similar. The methyl regions of the overtone spectra for 2,3,4,5,6-pentafluorotoluene and 2,3,5,6-tetrafluorotoluene are virtually identical with regard both to spectral pattern and to peak position. Compared with the overtone spectrum of 2,6-difluorotoluene, the methyl overtone spectra of 2,3,4,5,6-pentafluorotoluene and 2,3,5,6-tetrafluorotoluene are blue shifted. The aryl bands of 2,3,5,6-tetrafluorotoluene relative to 2,6-difluorotoluene blue shift more than the methyl bands.

The methyl overtone spectra of 3,5-difluorotoluene and toluene in Figures 1−5 are very different from the methyl overtone spectra of 2,3,4,5,6-pentafluorotoluene, 2,3,5,6-tetrafluorotoluene, and 2,6-difluorotoluene in Figures 6−10 except in the $\Delta v_{CH} = 2$ region (Figures 1 and 6), in which they are all similar. Compared with the methyl bands in Figures 2−5, the

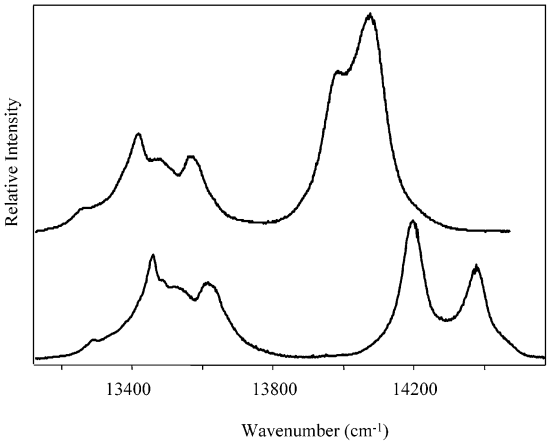

Figure 4. Room-temperature vapor phase overtone spectra of 3,5-difluorotoluene (bottom) and toluene (top) in the $\Delta v_{CH} = 5$ region. The spectra are rescaled to have similar magnitudes of methyl bands and are offset for clarity. The 3,5-difluorotoluene spectrum was measured by ICL-PAS with a pressure of 15 and 100 Torr of argon buffer gas. The toluene spectrum is taken from ref 35.

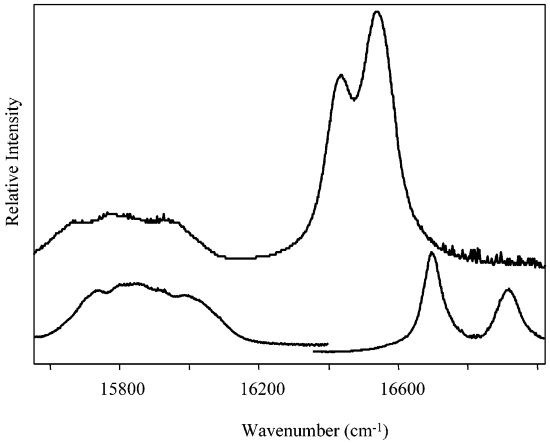

Figure 5. Room-temperature vapor phase overtone spectra of 3,5-difluorotoluene (bottom) and toluene (top) in the $\Delta v_{CH} = 6$ region. The spectra are rescaled to have similar magnitudes of methyl bands and are offset for clarity. The 3,5-difluorotoluene spectrum was measured by ICL-PAS with the dyes R6G and DCM and with a pressure of 15 and 100 Torr of argon buffer gas. The toluene spectrum is taken from ref 35.

higher energy parts of methyl bands in Figures 7−10 are weaker. In our previous work, we analyzed the similarities and differences of methyl band profiles between 2-, 3-, and 4-methylpyridines.[14] Differences in the methyl band profiles of 2-methylpyridine as compared to 3- and 4-methylpyridines arise from differences in the angular dependence of frequency and anharmonicity. The frequency changes, $\delta\tilde{\omega}$, and anharmonicity changes, $\delta\tilde{\omega}x$, for 3- and 4-methylpyridine are similar to each other but dissimilar to the changes for 2-methylpyridine.

We use the CH stretching methyl torsion model to analyze the methyl overtone spectra. The potential, frequency, and anharmonicity as a function of torsional angle (Table 1) are obtained as part of the procedure that we use to simulate the complex methyl regions of the overtone spectra.[13,14] We can observe from Table 1 that the constant parts of the frequencies gradually increase and the constant parts of anharmonicities gradually decrease from toluene to 3,5-difluorotoluene to 2,6-difluorotoluene to 2,3,5,6-tetrafluorotoluene to 2,3,4,5,6-pentafluorotoluene, which is consistent with the methyl band blue shifts in these molecules.

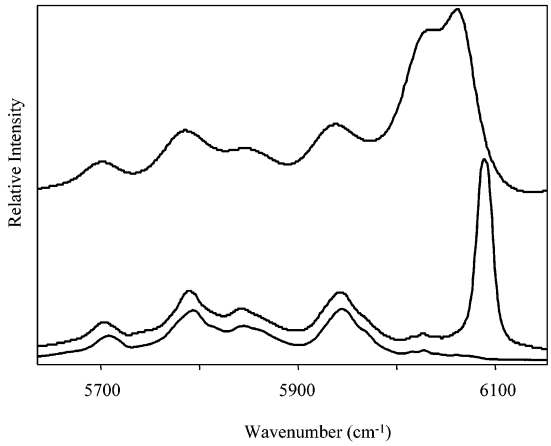

Figure 6. Room-temperature vapor phase overtone spectra of 2,3,4,5,6-pentafluorotoluene (bottom), 2,3,5,6-tetrafluorotoluene (middle), and 2,6-difluorotoluene (top) in the $\Delta v_{CH} = 2$ region. The spectra are rescaled to have similar magnitudes of methyl bands and are offset for clarity. The 2,3,5,6-tetrafluorotoluene spectrum and the 2,3,4,5,6-pentafluorotoluene spectrum were measured with a path length of 20.25 m and a pressure of 7 Torr. The 2,6-difluorotoluene spectrum is taken from ref 11.

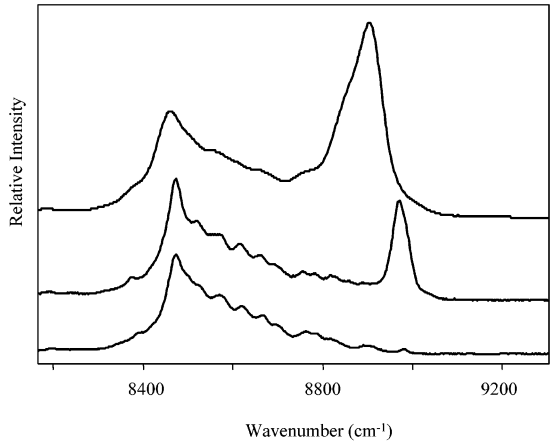

Figure 7. Room-temperature vapor phase overtone spectra of 2,3,4,5,6-pentafluorotoluene (bottom), 2,3,5,6-tetrafluorotoluene (middle), and 2,6-difluorotoluene (top) in the $\Delta v_{CH} = 3$ region. The spectra are rescaled to have similar magnitudes of methyl bands and are offset for clarity. The 2,3,5,6-tetrafluorotoluene spectrum and the 2,3,4,5,6-pentafluorotoluene spectrum were measured with a path length of 20.25 m and a pressure of 7 Torr. The 2,6-difluorotoluene spectrum is taken from ref 11.

From Table 1, the magnitudes of the $\cos(2\theta)$ terms of frequencies and anharmonicities for 2,6-difluorotoluene, 2,3,5,6-tetrafluorotoluene, and 2,3,4,5,6-pentafluorotoluene are similar and almost double the values for toluene and 3,5-difluorotoluene, which are also similar. The frequency and anharmonicity angular dependent terms have effects on the Hamiltonian that depend on v, the vibrational quantum number in the formula $[(v + 1/2)\delta\tilde{\omega} - (v + 1/2)^2\delta\tilde{\omega}x]$,[11,12] which explains the similarities and differences of methyl band profiles between these molecules. In the $\Delta v_{CH} = 2$ region, the frequency and anharmonicity angular dependent terms are relatively small and thus the differences between the methyl band profiles of these molecules in this region are much less (Figures 1 and 6) than those in the regions $\Delta v_{CH} > 2$ (Figures 2−5 and 7−10).

The torsional potentials of toluene and 3,5-difluorotoluene in Table 1 are smaller than those of 2,6-difluorotoluene, 2,3,5,6-tetrafluorotoluene, and 2,3,4,5,6-pentafluorotoluene and opposite in sign. Thus, in the geometry optimized structure, one methyl

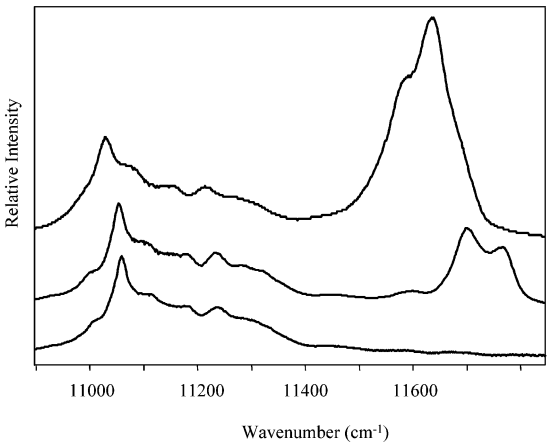

Figure 8. Room-temperature vapor phase overtone spectra of 2,3,4,5,6-pentafluorotoluene (bottom), 2,3,5,6-tetrafluorotoluene (middle), and 2,6-difluorotoluene (top) in the $\Delta v_{CH} = 4$ region. The spectra are rescaled to have similar magnitudes of methyl bands and are offset for clarity. The 2,3,5,6-tetrafluorotoluene spectrum and the 2,3,4,5,6-pentafluorotoluene spectrum were measured by ICL-PAS with a pressure of 11 Torr. The 2,6-difluorotoluene spectrum is taken from ref 11.

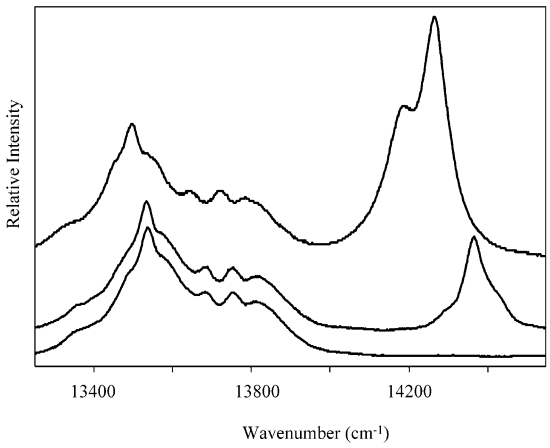

Figure 9. Room-temperature vapor phase overtone spectra of 2,3,4,5,6-pentafluorotoluene (bottom), 2,3,5,6-tetrafluorotoluene (middle), and 2,6-difluorotoluene (top) in the $\Delta v_{CH} = 5$ region. The spectra are rescaled to have similar magnitudes of methyl bands and are offset for clarity. The 2,3,5,6-tetrafluorotoluene spectrum was measured by ICL-PAS with a pressure of 13 Torr. The 2,3,4,5,6-pentafluorotoluene spectrum was measured by ICL-PAS with a pressure of 15 Torr. The 2,6-difluorotoluene spectrum is taken from ref 11.

CH bond is predicted to be in the benzene ring plane for toluene and 3,5-difluorotoluene while one methyl CH bond is perpendicular to the benzene ring plane for 2,6-difluorotoluene, 2,3,5,6-tetrafluorotoluene, and 2,3,4,5,6-pentafluorotoluene. However, the potentials of these molecules are so small the methyl groups are believed to rotate freely. The potentials V (see eq 19) of these molecules are small and are approximated to be independent of the quantum number v in the Hamiltonian. The slight differences in the torsional potentials are overshadowed by differences in the angular dependence of frequency and anharmonicity, which lead to the significant differences in methyl band profiles.

Comparison of the methyl band profiles of toluene and 2,6-difluorotoluene, and 3,5-difluorotoluene and 2,3,5,6-tetrafluorotoluene shows that fluorine substituents in the 2,6 positions cause the most significant change in the methyl band profiles, as one might have expected. Fluorine substituents at the 3,5 positions also cause methyl bands to blue shift, as evidenced

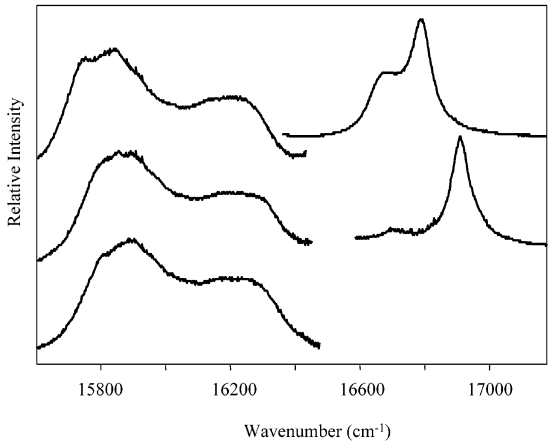

Figure 10. Room-temperature vapor phase overtone spectra of 2,3,4,5,6-pentafluorotoluene (bottom), 2,3,5,6-tetrafluorotoluene (middle), and 2,6-difluorotoluene (top) in the $\Delta v_{CH} = 6$ region. The spectra are rescaled to have similar magnitudes of methyl bands and the $\Delta v_{CH} = 6$ aryl band for 2,6-difluorotoluene and 2,3,5,6-tetrafluorotoluene, and are offset for clarity. The methyl region spectrum of 2,3,5,6-tetrafluorotoluene was measured with a pressure of 13 and 100 Torr of argon buffer gas. The aryl region spectrum of 2,3,5,6-tetrafluorotoluene was measured with a pressure of 16 and 100 Torr of argon buffer gas. The 2,3,4,5,6-pentafluorotoluene spectrum was measured with a pressure of 15 and 100 Torr of argon buffer gas. The spectra were measured by ICL-PAS with the dyes R6G and DCM. The 2,6-difluorotoluene spectrum is taken from ref 11.

by comparisons of the methyl bands of toluene and 3,5-difluorotoluene, and 2,6-difluorotoluene and 2,3,5,6-tetrafluorotoluene. A fluorine substituent in the 4 position has almost no effect on the methyl band profiles, as can be seen by a comparison of the methyl band profiles of 2,3,5,6-tetrafluorotoluene and 2,3,4,5,6-pentafluorotoluene.

Fermi resonance is observed in the aryl regions $\Delta v_{CH} = 2-4$ for 3,5-difluorotoluene (Figures 1−3), in the aryl region $\Delta v_{CH} = 4$ for 2,6-difluorotoluene, and in the aryl regions $\Delta v_{CH} = 4-6$ for 2,3,5,6-tetrafluorotoluene (Figures 8−10). For example, in the $\Delta v_{CH} = 4$ overtone, two peaks corresponding to the aryl CH bond of $CH_3C_6F_4\mathbf{H}$ are observed in Figure 8. We do not use the observed frequencies in the Birge−Sponer fit to obtain the frequency and anharmonicity of aryl CH stretching local modes. Rather we apply an analysis of a two-level system to obtain the unperturbed stretching frequencies, initially with eq 13 or 16. The calculations in Table 2 show that the differences between the unperturbed frequencies from eqs 13 and 16 are essentially zero. Therefore, we use the simpler eq 16 for the analysis. There are more than two peaks observed in the $\Delta v_{CH} = 4$ aryl region for the oscillators in the 2 and 6 positions of 3,5-difluorotoluene (Figure 3) and in the $\Delta v_{CH} = 4-5$ aryl regions for 2,3,5,6-tetrafluorotoluene (Figures 8 and 9). We simply analyze the two dominant peaks and ignore the other less intense ones (see eq 18).

Fermi resonances occur at the $\Delta v_{CH} = 2-4$ aryl bands for the 2,6 position oscillators and at the $\Delta v_{CH} = 3$ aryl bands for the 4 position oscillator in 3,5-difluorotoluene, at the $\Delta v_{CH} = 4$ aryl bands for the 3,5 position oscillators in 2,6-difluorotoluene, and at the $\Delta v_{CH} = 4-6$ aryl bands for the 4 position oscillator in 2,3,5,6-tetrafluorotoluene. Fluorine atom substitution causes neighboring stretching and bending frequency changes and thus affects the frequency match of the coupled states.

The unperturbed stretching frequencies (Table 2) have been fitted to the two-parameter Birge−Sponer equation (eq 3) to obtain local mode frequencies and anharmonicities for the aryl CH stretching oscillators. These frequencies and anharmonicities

TABLE 1: Calculated Potential, Frequency, and Anharmonicity (in cm^{-1}) as a Function of Torsional Angle for Toluene, 3,5-Difluorotoluene, 2,6-Difluorotoluene, 2,3,5,6-Tetrafluorotoluene, and 2,3,4,5,6-Pentafluorotoluene[a]

molecule	parameter	1	cos(θ)	cos(2θ)	cos(3θ)	cos(4θ)	cos(5θ)	cos(6θ)
toluene	V	−0.7	0.0	0.0	0.0	0.0	0.0	0.7
	Ω	3053.9	0.2	18.5	0.0	−0.8	−0.2	0.0
	X	59.9	0.0	−0.5	0.0	0.0	0.0	0.0
3,5-difluorotoluene	V	−1.3	0.0	0.0	0.0	0.0	0.0	1.3
	Ω	3064.5	0.2	18.8	0.0	−0.7	−0.2	0.0
	X	59.5	0.0	−0.5	0.0	0.0	0.0	0.0
2,6-difluorotoluene	V	7.0	0.0	0.0	−0.1	0.2	0.0	−7.1
	Ω	3081.8	0.3	34.7	0.0	1.1	−0.2	−0.2
	X	59.2	0.0	−1.0	0.0	−0.1	0.0	0.0
2,3,5,6-tetrafluorotoluene	V	6.0	0.0	0.0	−0.1	0.1	0.0	−6.0
	Ω	3088.8	0.2	33.3	0.0	1.0	−0.2	−0.1
	X	59.0	0.0	−0.9	0.0	−0.1	0.0	0.0
2,3,4,5,6-pentafluorotoluene	V	6.1	0.0	−0.1	−0.1	0.0	0.0	−5.9
	Ω	3089.7	0.2	32.4	0.0	1.1	−0.2	−0.5
	X	58.9	0.0	−0.9	0.0	−0.1	0.0	0.0

[a] The sixth-order Fourier series expansion coefficients for the potential (V), frequency (Ω), and anharmonicity (X), in cm^{-1} are calculated with the HF/6-31G(d) method. The calculated frequencies and anharmonicities have been scaled with the scaling factors 0.9377 and 0.907, respectively.[13]

TABLE 2: Fermi Resonance Analysis of the Observed Aryl CH Stretching Overtone Spectra of Vapor Phase 3,5-Difluorotoluene, 2,6-Difluorotoluene, and 2,3,5,6-Tetrafluorotoluene[a]

molecule	position	I_+	I_-	$\tilde{\nu}_+$[b]	$\tilde{\nu}_-$[b]	$\tilde{\nu}_1$[b]	$\tilde{\nu}_1$*[b]	$(\tilde{\nu}_1 - \tilde{\nu}_1^*)$[b]
3,5-difluorotoluene	2,6	1.961 27 × 10	1.53246 × 10	6 049.5	6 031.1	6 041.5	6 041.4	0.1
	2,6	3.098 45	1.38357	8 874.1	8 799.7	8 851.1	8 851.0	0.1
	4	2.674 36	1.78288	9 010.7	8 960.5	8 967.0	8 967.0	0.0
	2,6	3.694 50 × 10^{-3}	4.82635 × 10^{-3}	11 631.8	11 570.9	11 597.3	11 597.2	0.1
2,6-difluorotoluene	3,5	1.010 86 × 10^{-1}	6.84163 × 10^{-1}	11 686.6	11 639.8	11 645.8	11 645.8	0.0
2,3,5,6-tetrafluorotoluene	4	6.851 87 × 10^{-2}	1.36620 × 10^{-1}	11 766.3	11 702.4	11 723.8	11 723.7	0.1
	4	5.621 55 × 10^{-4}	1.24245 × 10^{-3}	14 417.3	14 363.6	14 380.3	14 380.3	0.0
	4	9.948 61 × 10^{-1}	5.43767 × 10^{-2}	16 910.1	16 704.2	16 899.4	16 899.3	0.1

[a] $\tilde{\nu}_1$ and $\tilde{\nu}_1$* are calculated from eqs 16 and 13, respectively. I_+ and I_- are integrated intensities from observed spectra. We only concentrate on the ratio within bands. [b] cm^{-1}.

TABLE 3: Local Mode Frequency and Anharmonicity (in cm^{-1}) of the Aryl CH Stretching Modes in Vapor Phase Toluene, 3,5-Difluorotoluene, 2,6-Difluorotoluene, and 2,3,5,6-Tetrafluorotoluene

		toluene[a]			3,5-difluorotoluene[b]		2,6-difluorotoluene[b]		2,3,5,6-tetrafluorotoluene[b]
	position:	2, 6[c]	3, 5[c]	4[c]	2, 6[d]	4[d]	3, 5[d]	4[c]	4[d]
obs	$\tilde{\omega}$	3144 ± 2	3170 ± 2	3170 ± 2	3192 ± 7	3218 ± 1	3205 ± 3	3189 ± 2	3218 ± 2
	$\tilde{\omega}x$	57.9 ± 0.3	59.1 ± 0.4	59.1 ± 0.4	58.6 ± 1.6	57.1 ± 0.3	58.4 ± 0.7	58.6 ± 0.5	57.2 ± 0.5
calc[e]	$\tilde{\omega}$	3148	3158	3162	3183	3208	3191	3177	3209
	$\tilde{\omega}x$	58.7	58.5	58.5	57.6	56.9	57.5	58.0	56.8

[a] From ref 35 and $\Delta_{CH} = 3-7$. [b] The observed frequency and anharmonicity are obtained from a fit of the local mode frequencies in the region $\Delta_{CH} = 2-6$. [c] Without Fermi resonance. [d] With Fermi resonance (Table 2). [e] With the HF/6-31G(d) method and the scaling factors from ref 13 with the structure obtained from geometry optimization.

of aryl CH stretching oscillators for toluene, 3,5-difluorotoluene, 2,6-difluorotoluene, and 2,3,5,6-tetrafluorotoluene are shown in Table 3 and compared to values calculated from ab initio theory. The ab initio frequencies and anharmonicities for all CH oscillators are scaled with scaling parameters from the aryl CH stretching oscillators of *p*-xylene.[13] The 4 position oscillators for 3,5-difluorotoluene and 2,3,5,6-tetrafluorotoluene and the 3,5 position oscillators for 2,6-difluorotoluene are all associated with Fermi resonance. The aryl CH oscillators for toluene and the 4 position oscillator for 2,6-difluorotoluene are not involved in Fermi resonance. However, the standard deviations from the fit of eq 3 for the observed frequencies and anharmonicities are similar for both sets. This verifies our Fermi resonance model. The standard deviations of the frequency and anharmonicity of the 2,6 position oscillators for 3,5-difluorotoluene are larger. The increased uncertainties are most probably due to uncertainties in the deconvolution procedure, since the aryl bands overlap the methyl bands in the $\Delta v_{CH} = 2$ and 3 regions.

The calculated frequencies of aryl CH oscillators in toluene decrease for CH bonds from the 4 position to the 3,5 positions and to the 2,6 positions in Table 3. The observed peaks corresponding to the 3,5 positions or the 4 position cannot be distinguished. The substituted fluorine atoms cause blue shifts in the aryl CH overtone spectra (Figures 1−10). For example, in 3,5-difluorotoluene, the 4 position CH oscillator is adjacent to two fluorine atoms whereas the CH oscillators at the 2,6 positions are adjacent to one fluorine atom and one methyl group and have a lower frequency. In 2,6-difluorotoluene, the frequency of the 3,5 position CH oscillators is higher than that of the 4 position CH oscillator.

A comparison of the 4 position CH oscillator frequencies for toluene and 3,5-difluorotoluene, and for 2,6-difluorotoluene and 2,3,5,6-tetrafluorotoluene in Table 3 indicates that it is the adjacent substituted fluorine atoms that cause a significant frequency increase. The 4 position CH oscillator frequency of 3,5-difluorotoluene is essentially the same as that of 2,3,5,6-tetrafluorotoluene. A comparison of the 3,5 position CH oscillator frequencies in 2,6-difluorotoluene and the 2,6 position CH oscillator frequencies in 3,5-difluorotoluene in Table 3 indicates that the methyl group causes the adjacent aryl CH

TABLE 4: Observed and Calculated Relative Oscillator Strengths for the CH Stretching Overtone Spectra of Vapor Phase 3,5-Difluorotoluene, 2,6-Difluorotoluene, and 2,3,5,6-Tetrafluorotoluene[a]

	3,5-difluorotoluene		2,6-difluorotoluene		2,3,5,6-tetrafluorotoluene	
	obs	calc[b]	obs	calc[b]	obs	calc[b]
$\|2\rangle_m$	0.57	0.53	0.52	0.50	0.69	0.71
$\|2\rangle_a$	0.43	0.47	0.48	0.50	0.31	0.29
$\|3\rangle_m$	0.56	0.56	0.53	0.49	0.81	0.77
$\|3\rangle_a$	0.44	0.44	0.47	0.51	0.19	0.23
$\|4\rangle_m$	0.49	0.56	0.44	0.48	0.71	0.79
$\|4\rangle_a$	0.51	0.44	0.56	0.52	0.29	0.21
$\|5\rangle_m$	0.53	0.56	0.52	0.48	0.80	0.78
$\|5\rangle_a$	0.47	0.44	0.48	0.52	0.20	0.22

[a] The subscripts m and a indicate methyl and aryl bands. [b] Calculated with the parameters in Tables 1 and 3.

oscillator frequency to red shift. The same result is obtained if we compare the 3,5 position CH oscillator frequencies and the 2,6 position CH oscillator frequencies in toluene.

It is difficult to measure the absolute intensity or to calculate the absolute intensity accurately. A comparison of the relative intensity of the total aryl to methyl band should minimize uncertainties introduced by our deconvolution procedure. We tried to deconvolute the spectrum of 2,6-difluorotoluene in the region $\Delta v_{CH} = 4$ with a different number of peaks but obtained the same relative aryl to methyl intensities in all cases. We also obtained the same relative intensities with deconvolutions whether we use a Gaussian profile or a Lorentzian profile. However, the slope of the baseline introduces error in the relative intensity. When severe overlapping occurs we cannot separate methyl bands from aryl bands. We subtract the highest energy peak of the methyl band from the aryl band for 2,6-difluorotoluene in the region $\Delta v_{CH} = 2$ and for 2,3,5,6-tetraflurotoluene in the region $\Delta v_{CH} = 4$ with an assumption of the same pattern for the methyl bands of 2,3,4,5,6-pentafluorotoluene, 2,3,5,6-tetrafluorotoluene, and 2,6-difluorotoluene. The relative oscillator strengths referred to the total oscillator strength in a given overtone of 3,5-difluorotoluene, 2,6-difluorotoluene, and 2,3,5,6-tetrafluorotoluene are given in Table 4.

If we assume the same intensity contribution from each methyl or aryl CH oscillator, then the expected ratio of aryl to methyl relative oscillator strengths should be 1:1 for 3,5-difluorotoluene and 2,6-difluorotoluene and 1:3 for 2,3,5,6-tetrafluorotoluene. We observe this general pattern from the observed and calculated relative oscillator strengths in Table 4.

The calculated relative oscillator strengths of aryl bands for 3,5-difluorotoluene are generally weaker than the methyl bands, as expected on an equal intensity basis. The observed relative oscillator strengths show a similar tendency except in the region $\Delta v_{CH} = 4$. The observed relative oscillator strengths of aryl bands for 2,6-difluorotoluene are weaker than the methyl bands except in the region $\Delta v_{CH} = 4$, as for 3,5-difluorotoluene. However, the calculated relative oscillator strengths of aryl bands for 2,6-difluorotoluene are opposite. In 2,3,5,6-tetrafluorotoluene the observed relative oscillator strengths of aryl bands are stronger than the expected 1:3 pattern in the regions $\Delta v_{CH} = 2$ and 4, while the calculated relative oscillator strength in the region $\Delta v_{CH} = 2$ confirms the observed relative oscillator strength. We observe unusually strong aryl bands in the region $\Delta v_{CH} = 4$ for 3,5-difluorotoluene, 2,6-difluorotoluene, and 2,3,5,6-tetrafluorotoluene. These are just the areas where Fermi resonance occurs. In our calculation only the stretching vibration is assumed to carry intrinsic oscillator strength. In cases of extensive Fermi resonance such as at $\Delta v_{CH} = 4$ this assumption likely leads to errors in the calculated oscillator strengths.

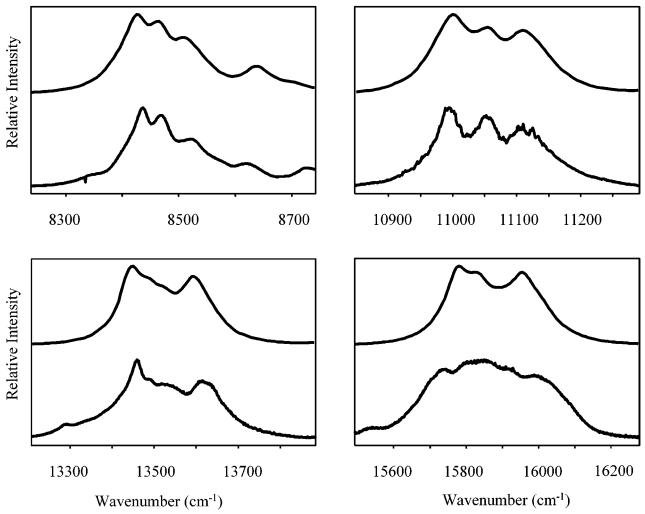

Figure 11. Observed (bottom) and simulated (top) spectra of 3,5-difluorotoluene in the methyl regions of $\Delta v_{CH} = 3-6$.

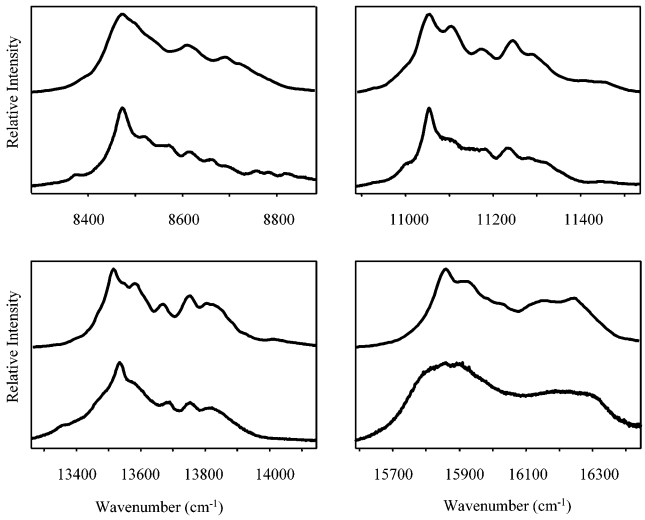

Figure 12. Observed (bottom) and simulated (top) spectra of 2,3,5,6-tetrafluorotoluene in the methyl regions of $\Delta v_{CH} = 3-6$.

One of the main goals in this work is to simulate the methyl regions of the CH stretching overtone spectra. We cannot obtain the parameters for the methyl group from the observed methyl band profiles directly. Rather, we can obtain the parameters ab initio and verify the parameters by the simulation. The simulation results are shown in Figures 11−13, where we have compared the observed and simulated methyl band profiles for 3,5-difluorotoluene, 2,3,5,6-tetrafluorotoluene, and 2,3,4,5,6-pentafluorotoluene from $\Delta v_{CH} = 3$ to 6. The simulation reproduced similarities and differences in the observed methyl profiles for these three molecules. However, the observed methyl band profiles of 2,3,5,6-tetrafluorotoluene and 2,3,4,5,6-pentafluorotoluene at $\Delta v_{CH} = 3$ have more spectral fine structure than the simulated spectra. Moreover, the simulated methyl bands are narrower than the observed bands in the spectra at $\Delta v_{CH} = 6$. This broadness is most likely caused by more efficient Intramolecular Vibrational Energy Redistribution (IVR) which is facilitated by Fermi resonance.[36]

In Figure 14, the simulated methyl band profiles of toluene are shown. In previous work we have also simulated these profiles at $\Delta v_{CH} = 2-5$ with a best fit procedure.[12] In the current work, we simulate the methyl band profiles of toluene at $\Delta v_{CH} = 3-6$ with 340 points from ab initio calculations. In our

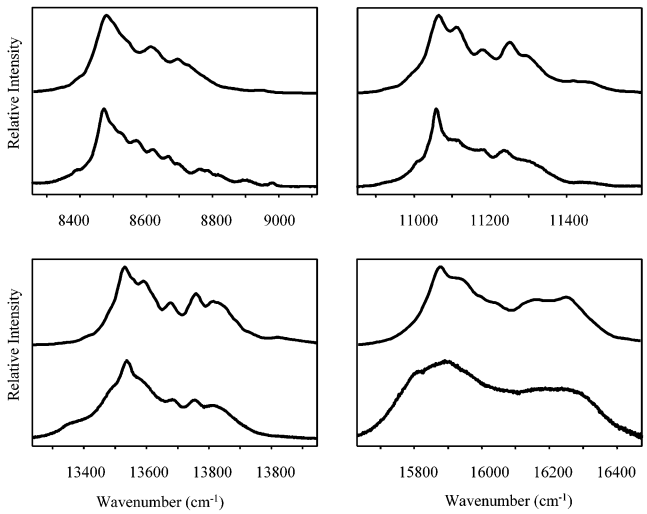

Figure 13. Observed (bottom) and simulated (top) spectra of 2,3,4,5,6-pentafluorotoluene in the methyl regions of $\Delta v_{CH} = 3-6$.

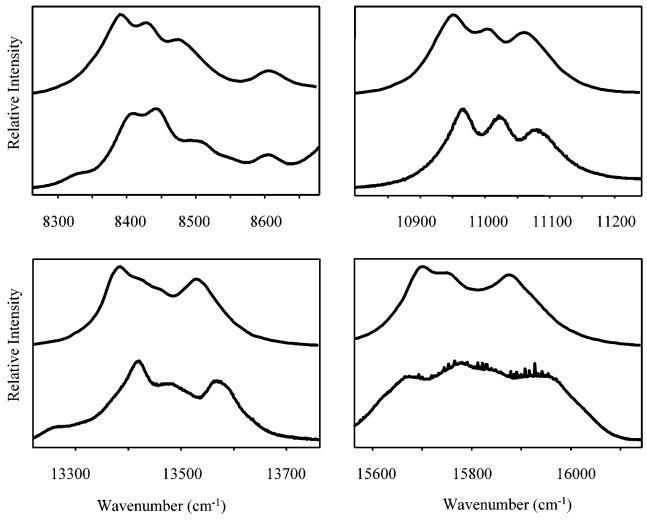

Figure 14. Observed (bottom) and simulated (top) spectra of toluene in the methyl regions of $\Delta v_{CH} = 3-6$. Observed spectra are from ref 35.

previous work we could not reproduce the peak around 8600 cm^{-1} at $\Delta v_{CH} = 3$.[12] We expanded the dipole moment function to the second order for the cross term in a Taylor series as a function of the displacement coordinates in our previous work.[12] Here we include the dipole moment function to the third-order mixed terms depending on two CH stretching coordinates such as $q_1 q_2^2$ and $q_1^2 q_2$ terms. This addition is the likely cause of the improved simulation.

In Figure 15, we simulate the methyl band profiles of 2,6-difluorotoluene, which were simulated previously.[11] Comparing Figure 15 and the simulated results in ref 11, we find that our current, more general approach leads to improvements in the simulation.

Conclusion

We have measured the room-temperature vapor phase overtone spectra of 3,5-difluorotoluene, 2,3,5,6-tetrafluorotoluene, and 2,3,4,5,6-pentafluorotoluene with conventional absorption spectroscopy and intracavity laser photoacoustic spectroscopy in the regions corresponding to $\Delta v_{CH} = 2-6$. The relative oscillator strengths of the aryl band to the methyl band at $\Delta v_{CH} = 2-5$ have been measured and calculated.

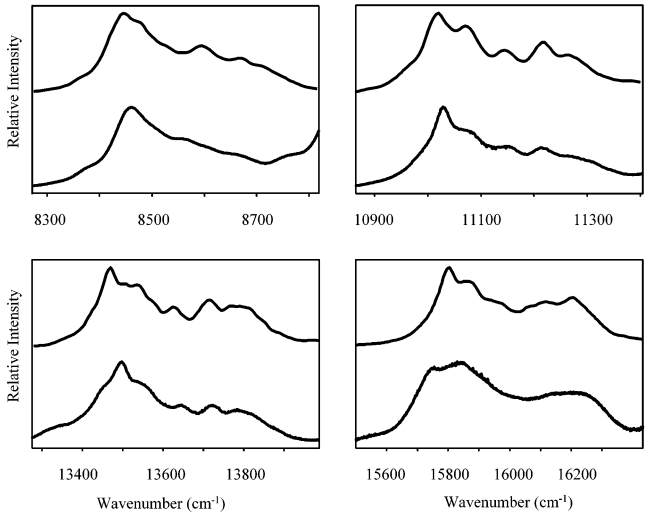

Figure 15. Observed (bottom) and simulated (top) spectra of 2,6-difluorotoluene in the methyl regions of $\Delta v_{CH} = 3-6$. Observed spectra are from ref 11.

We have used expressions for a two-level system model to obtain the unperturbed aryl CH stretching frequencies from the perturbed frequencies and relative oscillator strengths. From these data, we have obtained aryl CH stretching local mode frequencies and anharmonicities for 3,5-difluorotoluene, 2,6-difluorotoluene, and 2,3,5,6-tetrafluorotoluene.

We have used the CH stretching methyl torsion model to simulate the methyl band profiles of toluene, 3,5-difluorotoluene, 2,6-difluorotoluene, 2,3,5,6-tetrafluorotoluene, and 2,3,4,5,6-pentafluorotoluene. We have successfully reproduced the observed methyl band profiles for these fluorine substituted toluenes.

We have noted chemical environmental effects on the overtone spectra of the aryl CH oscillators and methyl groups in toluene, 3,5-difluorotoluene, 2,6-difluorotoluene, 2,3,5,6-tetrafluorotoluene, and 2,3,4,5,6-pentafluorotoluene. Fluorine substituents shift the methyl bands to higher energy. Fluorine substituents at the 2,6 positions significantly affect the methyl band profiles whereas fluorine substituents at the 3,5 positions have a limited effect on the spectral positions, as expected. The effect of the fluorine substitutents at the 4 position is negligible. The aryl CH stretching overtone spectra are primarily affected by the nearest neighboring substituents, as expected.

Acknowledgment. Funding for this research has been provided by the Natural Sciences and Engineering Research Council of Canada.

References and Notes

(1) Hayward, R. J.; Henry, B. R. *J. Mol. Spectrosc.* **1975**, *57*, 221.
(2) Henry, B. R. *Acc. Chem. Res.* **1977**, *10*, 207.
(3) Watson, I. A.; Henry, B. R.; Ross, I. G. *Spectrochim. Acta A* **1981**, *37*, 857.
(4) Child, M. S.; Lawton, R. T. *Faraday Discuss. Chem. Soc.* **1981**, *71*, 273.
(5) Child, M. S.; Halonen, L. *Adv. Chem. Phys.* **1984**, *57*, 1.
(6) Henry, B. R.; Hung, I. F. *Chem. Phys.* **1978,** *29*, 465.
(7) Mortensen, O. S.; Henry, B. R.; Mohammadi, M. A. *J. Chem. Phys.* **1981,** *75*, 4800.
(8) Sheppard, N.; Woodman, C. M. *Proc. R. Soc. London, Ser. A* **1969**, *313*, 149.
(9) Anastasakos, L.; Wildman, T. A. *J. Chem. Phys.* **1993**, *99*, 9453.
(10) Cavagnat, D.; Lespade, L.; Lapouge, C. *J. Chem. Phys.* **1995**, *103*, 10502.
(11) Zhu, C.; Kjaergaard, H. G.; Henry, B. R. *J. Chem. Phys.* **1997**, *107*, 691.

(12) Kjaergaard, H. G.; Rong, Z.; McAlees, A. J.; Howard, D. L.; Henry, B. R. *J. Phys. Chem. A* **2000**, *104*, 6398.
(13) Rong, Z.; Kjaergaard, H. G. *J. Phys. Chem. A* **2002**, *106*, 6242.
(14) Rong, Z.; Kjaergaard, H. G.; Henry, B. R. *J. Phys. Chem. A* **2002**, *106*, 4368.
(15) Rong, Z.; Howard, D. L.; Kjaergaard, H. G. *J. Phys. Chem. A* **2003**, *107*, 4607.
(16) Proos, R. J.; Henry, B. R. *J. Phys. Chem. A* **1999**, *103*, 8762.
(17) Duncan, J. L.; Ellis, D.; Wright, I. J. *Mol. Phys.* **1971**, *20*, 673.
(18) Dübal, H.; Quack, M. *J. Chem. Phys.* **1984**, *81*, 3779.
(19) Perry, J. W.; Moll, D. J.; Kuppermann, A.; Zewail, A. H. *J. Chem. Phys.* **1985**, *82*, 1195.
(20) Crofton, M. W.; Stevens, C. G.; Klenerman, D.; Gutow, J. H.; Zare, R. N. *J. Chem. Phys.* **1988**, *89*, 7100.
(21) Niefer, B. I.; Kjaergaard, H. G.; Henry, B. R. *J. Chem. Phys.* **1993**, *99*, 5682.
(22) Hegelund, F.; Mäder, H.; Wiemeler, M.; Winther, F. *J. Mol. Spectrosc.* **1995**, *171*, 22.
(23) Winther, F.; Schönhoff, M. *J. Mol. Spectrosc.* **1997**, *186*, 54.
(24) Sowa, M.; Henry, B. R. *J. Chem. Phys.* **1991**, *95*, 3040.
(25) Henry, B. R.; Sowa, M. G. *Prog. Anal. Spectrosc.* **1989**, *12*, 349.
(26) Henry, B. R.; Kjaergaard, H. G.; Niefer, B.; Schattka, B. J.; Turnbull, D. M. *Can. J. Appl. Spectrosc.* **1993**, *38*, 42.
(27) GRAMS AI is commercially available software from Thermo Galactic.
(28) Atkins, P. W. *Molecular Quantum Mechanics*, 2nd ed.; Oxford University: Oxford, U.K., 1983.
(29) Birge, R. T.; Sponer, H. *Phys. Rev.* **1926**, *28*, 259.
(30) Sowa, M. G.; Henry, B. R.; Mizugai, Y. *J. Phys. Chem.* **1991**, *95*, 7659.
(31) Low, G. R.; Kjaergaard, H. G. *J. Chem. Phys*. **1999**, *110*, 9104.
(32) Daub, C. D.; Henry, B. R.; Sage, M. L.; Kjaergaard, H. G. *Can. J. Chem*. **1999**, *77*, 1775.
(33) Frisch, M. J.; Trucks, G. W.; Schlegel, H. B.; Scuseria, G. E.; Robb, M. A.; Cheeseman, J. R.; Zakrzewski, V. G.; Montgomery, J. A., Jr.; Stratmann, R. E.; Burant, J. C.; Dapprich, S.; Millam, J. M.; Daniels, A. D.; Kudin, K. N.; Strain, M. C.; Farkas, O.; Tomasi, J.; Barone, V.; Cossi, M.; Cammi, R.; Mennucci, B.; Pomelli, C.; Adamo, C.; Clifford, S.; Ochterski, J.; Petersson, G. A.; Ayala, P. Y.; Cui, Q.; Morokuma, K.; Malick, D. K.; Rabuck, A. D.; Raghavachari, K.; Foresman, J. B.; Cioslowski, J.; Ortiz, J. V.; Stefanov, B. B.; Liu, G.; Liashenko, A.; Piskorz, P.; Komaromi, I.; Gomperts, R.; Martin, R. L.; Fox, D. J.; Keith, T.; Al-Laham, M. A.; Peng, C. Y.; Nanayakkara, A.; Gonzalez, C.; Challacombe, M.; Gill, P. M. W.; Johnson, B.; Chen, W.; Wong, M. W.; Andres, J. L.; Gonzalez, C.; Head-Gordon, M.; Replogle, E. S.; Pople, J. A. *Gaussian98*, Revision A.5; Gaussian, Inc.: Pittsburgh, PA, 1998.
(34) Herzberg, G. *Molecular Spectra and Molecular Structure, II. Infrared and Raman Spectra of Polyatomic Molecules*; D. Van Nostrand Company, Inc.: New York, 1968.
(35) Kjaergaard, H. G.; Turnbull, D. M.; Henry, B. R. *J. Phys. Chem.* **1997**, *101*, 2589.
(36) Petryk, M. W. P.; Henry, B. R. *J. Phys. Chem. A* **2002**, *106*, 8599.